Hydrogen-induced lattice rearrangement of a $Pd_{0.81}Au_{0.19}$ alloy

Hydrogen-induced lattice rearrangement of a Pd$_{0.81}$Au$_{0.19}$ alloy

S-M Lee[1], H Noh[2], Ted B Flanagan[2] and S Luo[2]

[1] Department of Materials Engineering, KangWon National University, Chuncheon, Kangwon Do 200-701, Korea
[2] Chemistry Department, University of Vermont, Burlington, VT 05405, USA

Abstract

At moderate temperatures and H$_2$ pressures, e.g., $\geqslant$423 K and $\geqslant$5 bar, an fcc solid solution Pd$_{0.81}$Au$_{0.19}$ alloy is shown to form a hydrogen-stabilized, ordered phase. The dissolved hydrogen plays two roles during hydrogen heat treatment (HHT): (i) a kinetic role in enhancing the metal atom rearrangement leading to ordering and (ii) an equilibrium role in shifting the equilibrium from a disordered to an H-stabilized ordered alloy. The H-induced changes are followed by diagnostic H$_2$ isotherms, usually measured at 348 K.

The hydrogen solubilities found in the diagnostic isotherms (348 K) are greatest for alloys which have been treated with hydrogen at the highest p_{H_2} for the longest times at moderate temperatures, e.g., 473 K, where the H solubilities and H-assisted metal atom diffusivities are both appreciable. Thermodynamic parameters for hydrogen solution in the alloy before and after HHT have been determined from equilibrium pressure–composition–temperature data and calorimetry.

Dissolved H is shown to stabilize the ordered state because, at the same temperature where ordering occurs, but in the absence of dissolved H, the alloy returns to its disordered form. Dissolved H is shown to assist metal atom diffusion because the return of the ordered form to a nearly disordered state characteristic of 1 MPa is faster in the presence of H$_2$ than *in vacuo*.

1. Introduction

Bulk Pd–Au alloys form a continuous series of fcc solid solutions at high temperatures; however, evidence for long range order has been reported at lower temperatures for the compositions Pd$_3$Au and PdAu$_3$ [1]. There is firmer evidence for the existence of short range order at certain compositions [2]. Kohl *et al* [3] reported from resistivity studies of the X_{Au} = 0.9, 0.75 and 0.5 alloys that short range order occurs at these compositions. They measured activation energies for mobility and enthalpies for vacancy formation; for the

$X_{Au} = 0.5$ alloy the activation energy for mobility is $E_m = 1.35$ eV and the enthalpy of vacancy formation is $\Delta H_f = 1.37$ eV.

Kawasaki *et al* [4] reported that in evaporated films of Pd–Au alloys an $L1_2$ super-lattice appears within the composition range from $X_{Au} = 0.17$ to 0.26 following annealing at 873 K for 10 h. After annealing at similar temperatures for periods up to 20 days they were unable to detect any evidence for super-lattice reflections in bulk alloys of similar compositions. They concluded that the times for metal atom diffusion were too long for the establishment of order in the bulk alloys. This would appear to be unlikely since it would be expected that annealing at 873 K for 10–20 days would be sufficient for long range order to be established. The enthalpies of mixing [5] to form solid solutions of these alloys are exothermic, which favours ordering. There appear to be no further experimental reports of ordering in these alloys, except for a brief account concerning some of the work to be described here for the H-stabilized ordering of the $X_{Au} = 0.19$ alloy [6]. In this work the HHT (hydrogen heat treatment) has been extended to higher p_{H_2} and thermodynamic parameters have been determined for the HHTed (H-heat treated) alloys.

As in pure Pd, H is believed to occupy the octahedral interstices in Pd alloys. This has been supported by Lovvik and Olsen [7] from density functional calculations for Pd–Ag alloys. Hydrogen solubility in Pd–Au alloys has been investigated by Allard *et al* [8] and Shamsuddin and Kleppa [9]. Substitutional Au expands the Pd lattice and the solution of H_2 becomes more exothermic with increase of X_{Au}, but the hydrogen capacity of the alloys, i.e. the hydrogen content reached at moderately high pressures, decreases with X_{Au}. It seems from the entropy values that hydrogen occupies octahedral interstices selectively, in keeping with the Mössbauer results of Wagner *et al* [10].

It has been found that dissolved hydrogen causes certain palladium alloys to undergo lattice changes at temperatures where these changes do not occur *in vacuo* [11–13]. It is of interest to subject the bulk form of a disordered Pd–Au alloy to a hydrogen heat treatment (HHT) to learn if it undergoes ordering. It has been observed that dissolved hydrogen causes disordered Pd_3Mn to order at temperatures, e.g. 523 K, where ordering does not occur at measurable rates *in vacuo* [14, 15] and, in addition, the presence of the dissolved H leads to the $L1_2$ ordered form rather than to the long period superstructure (lps) of the Al_3Zr-type which forms *in vacuo* [16]. Dissolved H stabilizes the $L1_2$ form of Pd_3Mn as shown by its reversion to the lps form when heated *in vacuo* at the same temperature at which it formed the $L1_2$ structure. The lattice changes are reflected in the changes of the hydrogen isotherms at moderate temperatures and p_{H_2} because the hydrogen solubility is very sensitive to the detailed lattice structure. The hydrogen solubility was found to be greater in the $L1_2$ form than the disordered or lps form. The fact that the $L1_2$ ordered form resulted from HHT was established from electron diffraction. Neutron diffraction patterns of deuterated Pd_3Mn established that the Pd-rich interstices, Pd_6, are occupied preferentially, and in the $L1_2$ form these are occupied almost 100%, whilst the others are empty at the D content of $D/M \approx 0.25$ corresponding to ≈ 0.1 MPa [17]. It seems that many workers are unaware of the great sensitivity of H_2 solubilities for lattice changes in Pd based alloys, e.g., [18, 19].

Wagner *et al* [10] found from Mössbauer spectroscopy that substitutional Au atoms in Pd repel H atoms more strongly than any of the other substitutional metals which they investigated, except for Sn, which acts similarly. If even one Au atom was amongst the six closest metal atoms surrounding the octahedral interstice, the interstice was not occupied by hydrogen, according to Wagner *et al*. This means that Pd–Au alloys are well suited for following lattice changes with hydrogen solubilities since the solubilities will be strongly affected by the nearest neighbour environment of the interstices. For example, it is expected that ordering will lead

to a greater fraction of Pd_6 interstices, i.e., those surrounded by Pd nearest neighbours, as in $L1_2$-Pd_3Mn.

In the present study $Pd_{0.81}Au_{0.19}$ alloys will be exposed to H_2 at moderately high temperatures and at p_{H_2} up to 100 MPa in order to learn if any lattice changes occur. This composition was selected because it is close to the average composition where Kawasaki *et al* [4] observed a superstructure in Pd–Au thin films. 'Diagnostic' isotherms measured at a lower temperature before and after the hydrogen heat treatment, HHT, will be employed to monitor any lattice changes which occur and, if changes occur, the transformed alloys will be examined by physical means, e.g., x-ray diffraction (XRD), transmission electron microscopy (TEM) and electron diffraction.

2. Experimental details

The $Pd_{0.81}Au_{0.19}$ alloys were initially in the form of thin sheets supplied by Engelhard Corp., and these were cold-rolled and annealed *in vacuo* at 1173 K for 5 h to form the disordered alloy. The alloys were fcc with a larger lattice parameter than Pd and the annealed alloys showed no evidence for any super-lattice formation from x-ray diffraction. That is, significant ordering does not result from the annealing and slow cooling, as shown from XRD and also because there was no significant difference in H_2 isotherms (348 K) between alloys which were slowly cooled in the furnace or quenched from the annealing temperature.

After HHT, the hydrogen was quickly evacuated at the elevated temperature, cooled, and a 'diagnostic' isotherm was measured at 348 K in order to learn whether or not any lattice changes had occurred. It is important to distinguish between the temperatures of HHT and the temperature of the diagnostic isotherms; the latter is low compared to the temperatures employed for HHT and therefore ordering or disordering will not occur at the temperature of the diagnostic isotherms, at least at the p_{H_2} employed.

H_2 pressures up to 100 MPa were employed for the HHT. Analytical techniques helped to characterize the alloy after HHT, e.g., XRD, TEM, and electron microprobe analysis. TEM was carried out using a JEOL 40000FX electron microscope operating at 400 kV.

Enthalpies of H_2 solution were determined from p–c–T (p_{H_2}–concentration–temperature) relationships and also directly from reaction calorimetry for both the ordered and disordered $Pd_{0.81}Au_{0.19}$ alloy (303 K). The calorimeter has been described elsewhere [20].

3. Results and discussion

3.1. Examination by XRD and TEM

The authors have previously reported from electron diffraction studies that after HHT of an initially disordered fcc $Pd_{0.81}Au_{0.19}$ alloy some H-stabilized order occurs [6].

After being subjected to HHT (20 h at 7.0 MPa at 473 K), the lattice parameter of the $Pd_{0.81}Au_{0.19}$ alloy was found to have not changed significantly, $a_\circ = 0.3926$ nm, which is in good agreement with parameters for these disordered alloys found earlier [21]. Normally the ordered forms of alloys have smaller lattice constants than the corresponding disordered forms [22], but this is not discernable in the present case, perhaps because the ordering was incomplete. Additional peaks appeared in the x-ray diffraction pattern of the $Pd_{0.81}Au_{0.19}$ alloy after it had been subjected to HHT for a long period of time, 383 h, at 7.0 MPa (423 K); the presence of extra reflections is, of course, a characteristic of super-lattices; however, they were not found after HHT at higher H_2 pressures but for shorter times.

TEM examination of the alloys after HHT revealed super-lattice phases as also found earlier [6]; such regions *were never observed in the alloy not subjected to HHT*. TEM studies
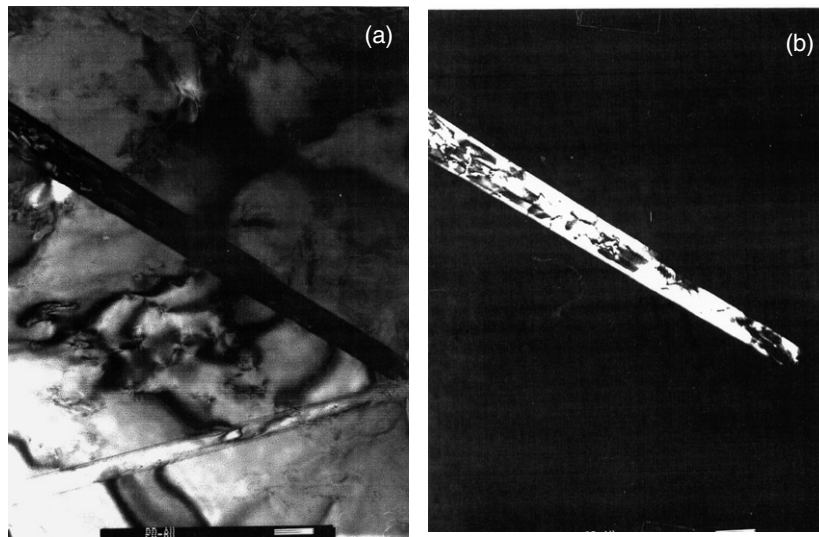
Figure 1. TEM photographs of HHTed (100 MPa, 473 K, 4 h) $Pd_{0.81}Au_{0.19}$ showing a long needle-like super-lattice phase. (a) The bright field electron diffraction pattern, (b) the dark field pattern of the same super-lattice phase as shown in (a).
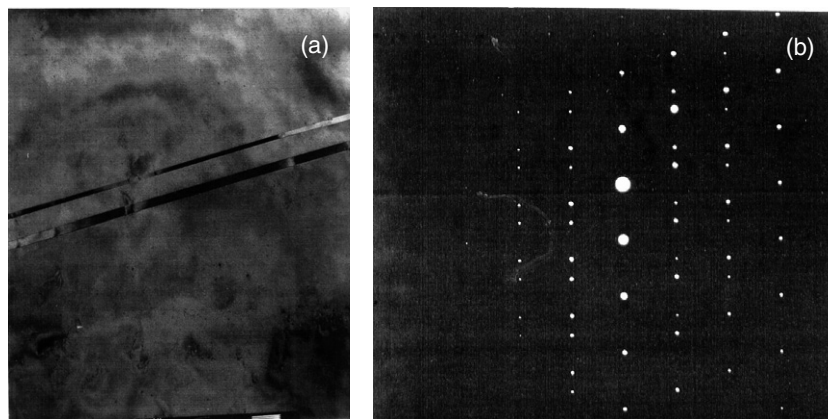
Figure 2. Photomicrograph of (a) twins and (b) an electron diffraction pattern of the long range ordered phase of the $Pd_{0.81}Au_{0.19}$ alloy after HHT at 100 MPa, 473 K, 4 h.

were carried out in this work for alloys subjected to HHT at 100 MPa for 4 h (473 K). Again super-lattice phase was found (figure 1) having the same electron diffraction pattern as found previously [6] but, in addition, there were many twins (figure 2(a)). The structure of the super-lattice phase appears not to be $L1_2$ as expected, but more complex and, because the necessary patterns for zone axes with low indices were not available, the structure was not determined here. In any case, the presence of extra reflections demonstrates the presence of a super-lattice phase (figure 2(b)). EDS analysis showed that there is no significant difference between the composition of the super-lattice phase and the matrix, indicating ordering rather than segregation has occurred.

A grain (2 μm) of an HHTed $Pd_{0.81}Au_{0.19}$ alloy (7.0 MPa, 473 K, 20 H) was examined using SADP (selected area diffraction patterns), and from the presence of modulated diffraction
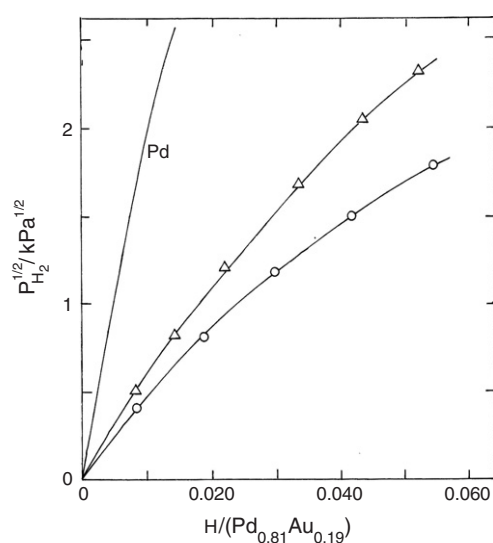
Figure 3. H_2 solubilities in the dilute region (348 K). $\triangle$, annealed $Pd_{0.81}Au_{0.19}$ alloy; O, HHTed at 100 MPa, 473 K $Pd_{0.81}Au_{0.19}$ alloy.

patterns it was apparent that there was short range order over the whole grain. In addition, there was a plate-like super-lattice phase which had grown within the grain. Some short-range order was also observed in the annealed alloys but, again, the super-lattice phases were only observed in the HHT alloys.

The dislocation density of the $Pd_{0.81}Au_{0.19}$ alloy subjected to HHT (10 MPa, 523 K) was only slightly greater than that of the annealed alloy and the dislocations were located mainly at the interface between the super-lattice and surrounding matrix phases. There should be no increase of hydrogen solubility due to dislocation trapping of H because of the observed low dislocation density.

3.2. Diagnostic isotherms of the Pd/Au alloy after HHT

3.2.1. General considerations. Many experiments were carried out in which disordered $Pd_{0.81}Au_{0.19}$ alloys were exposed to H_2 at various p_{H_2} values and temperatures for different periods of time. The HHT temperatures ranged from 373 to 523 K and the p_{H_2} employed was up to 100 MPa. Generally the hydrogen diagnostic isotherms of the alloy were measured at 348 K before and after HHT and the solubilities were found to increase with time of the HHT exposure and with p_{H_2}, and showed a maximum effect of temperature after HHT at $\approx$473 K. It should be noted that the H in the alloys leading to ordering is rapidly removed by evacuation at elevated temperatures before cooling, and the diagnostic isotherm measurements are made with the resulting H-free alloys. The changes of hydrogen solubilities after HHT as reflected by the diagnostic isotherms are most likely caused by H-enhanced metal atom diffusion, leading to lattice changes.

3.2.2. Dilute phase hydrogen solubility after HHT. The dilute phase solubilities (348 K) for the $Pd_{0.81}Au_{0.19}$ alloy before and after HHT at 100 MPa for 5 h (473 K) are shown in figure 3. It is clear that there is a substantially greater hydrogen solubility after HHT. The solubility for the HHTed (H-heat treated) alloy intersects the origin and behaves ideally, i.e., follows Sieverts'
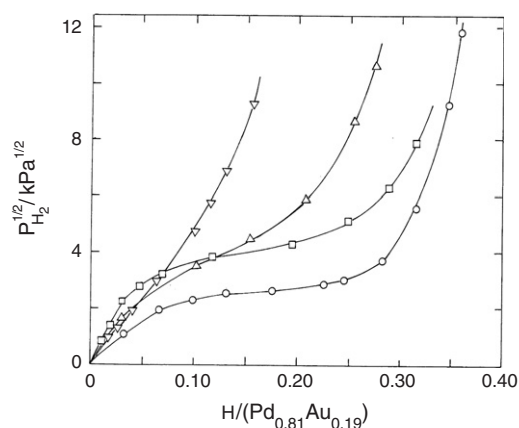
Figure 4. Diagnostic isotherms (348 K) for disordered and HHTed Pd–Au alloys. ▽, disordered $Pd_{0.73}Au_{0.27}$; △, disordered $Pd_{0.81}Au_{0.19}$; □, disordered $Pd_{0.85}Au_{0.15}$; O, the $Pd_{0.81}Au_{0.19}$ alloy HHTed at 100 MPa, 473 K.

law at low H contents, $(H/M) = K_s\, p_{H_2}^{1/2}$, indicating an absence of strong trapping of H. For comparison, data are shown for annealed Pd–H [23], where it is clear that there is a greater dilute phase solubility for the alloy.

3.2.3. Representative complete diagnostic isotherms before and after HHT.　　Figure 4 shows diagnostic isotherms (348 K) for the $Pd_{0.81}Au_{0.19}$ alloy before and after HHT in comparison to isotherms for disordered $X_{Au} = 0.15$ and 0.26 alloys. The isotherm for the disordered $Pd_{0.81}Au_{0.19}$ alloy does not have a two phase, invariant pressure region and, as expected, its isotherm lies between the $X_{Au} = 0.15$ and 0.26 alloys, but, following HHT (473 K, 100 MPa, 10 h), its isotherm no longer falls between these two but exhibits a greater solubility than either.

It does not seem possible to attribute the diagnostic isotherm after HHT to separation into Pd-poor and Pd-rich phases as occurs for the Pd–Rh and Pd–Pt alloys after HHT [13, 24]. The plateau-like behaviour and the relatively large H capacity cannot be due to the formation of alloy phases with $X_{Au} > 0.19$ because they would have smaller capacities without a plateau-like region (see $X_{Au} = 0.26$ in figure 4). If the behaviour is mainly due to an alloy phase with $X_{Au} < 0.19$, it would have a plateau with a greater pressure than that observed (figure 4), and furthermore the dilute phase behaviour of the alloy after HHT does not correspond to alloys with $X_{Au} < 0.19$ because their dilute phase solubilities are greater than the observed one.

It has been shown from thermodynamic arguments by Park and Flanagan [26] that alloys with plateau pressures lower than Pd would not be expected to separate into two phases under HHT because this will not lead to a lowering of the system free energy. The Pd–Au system is a borderline case where the plateau pressures do not change very much from that of Pd–H upon alloying with Au. The relatively low temperature where the HHT changes occur, e.g. 348 K, suggests ordering rather than segregation, since ordering does not require long range diffusion, in contrast to segregation.

For the Pd–Rh and Pd–Pt alloys, H-induced segregation into Pd-rich and Pd-poor phases takes place at ⩾623 K and ⩾448 K, respectively [13, 24]. EDS analysis of the HHTed $Pd_{0.81}Au_{0.19}$ alloy revealed no significant differences in composition between the region believed to be ordered and the matrix. It has been found previously that ordering significantly increases hydrogen solubilities in Pd_3Fe [27] and Pd_3Mn [15]. An exception is Pd_7Ce, where
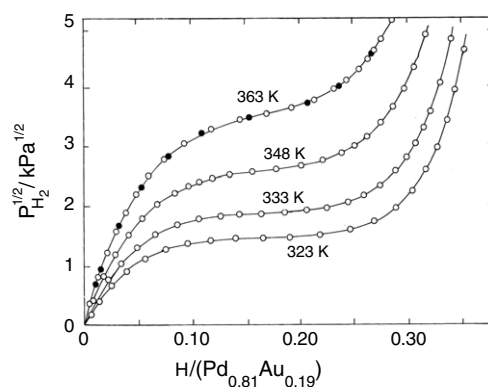
Figure 5. Diagnostic isotherms for different temperatures for the HHTed $Pd_{0.81}Au_{0.19}$ alloy (100 MPa, 10 h, 473 K). The open and filled symbols are for absorption and desorption, respectively.

there is a slight decrease of solubility in the ordered form, although both solubilities are small [28]. In view of the large increases in solubility in the $Pd_{0.81}Au_{0.19}$ alloy after HHT, it seems reasonable to assume that the origin of the increased H solubility is ordering. This is corroborated by physical analytical measurements, e.g. TEM, where the super-lattice phases only appear after HHT. Although the HHTed alloy does not seem to have complete long range order, it will be referred to, for convenience, as ordered.

The role of the observed short range order on the H_2 solubility is unknown; however, the solubilities after slow cooling or rapid quenching of the alloy from 1173 K give similar H_2 diagnostic isotherms, indicating either that short range order is established under both conditions are else it is not a factor in the solubility.

3.2.4. Thermodynamic parameters for H_2 solution in the $Pd_{0.81}Au_{0.19}$ alloy before and after HHT. It is useful to determine thermodynamic parameters for H_2 solution in a $Pd_{0.81}Au_{0.19}$ alloy before and after HHT because this gives some insight into the changes which have occurred. With increase in the degree of HHT, the diagnostic isotherms become more horizontal, resembling a two phase, plateau region. In figure 5 absorption isotherms are shown at four different temperatures (323–363 K) for the $Pd_{0.81}Au_{0.19}$ alloy after HHT (473 K, 100 MPa, $\approx$10 h). At 363 K the desorption isotherm was also measured, which agrees very well with the absorption one, indicating an absence of hysteresis and also attesting to the accuracy of the data, because errors in the volumes of the measuring apparatus can introduce a cumulative error in the results which would be reflected by a lack of correspondence of the H contents for the absorption and desorption data. The isotherm at 323 K appears to be very close to one for a critical temperature, indicating a miscibility gap. The critical composition X_{Au} where the hydride phase no longer forms for disordered alloys is 0.16 at 298 K [8], and at 323 K it will be somewhat lower.

Relative partial molar thermodynamic parameters for the reaction

$$\tfrac{1}{2}H_2(0.1 \text{ MPa, g}) \rightarrow [H]_r \qquad (1)$$

were obtained from H_2 isotherms at different temperatures [29], where $[H]_r$ represents hydrogen dissolved in the alloy at a given value of $r = H/(Pd_{0.81}Au_{0.19})$. The relationship between the equilibrium p_{H_2} and the relative partial molar enthalpy and entropy change for
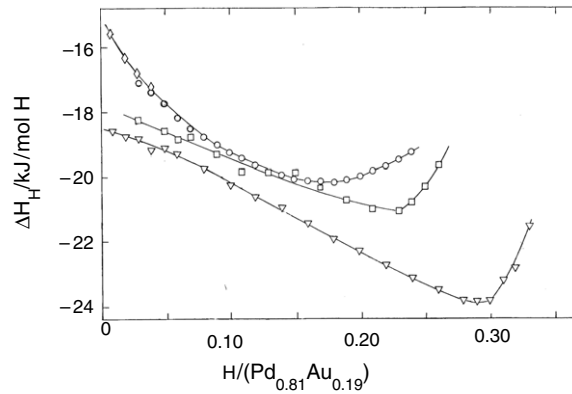
Figure 6. ΔH_H as a function of $r = (H/(Pd_{0.81}Au_{0.19})$ for several forms of the alloy derived from isotherms e.g.: figure 5. O, annealed and slowly cooled, $Pd_{0.81}Au_{0.19}$; ◇, quenched from 1173 K; □, HHTed (10.8 MPa, 473 K, 62 h); ▽, HHTed (100 MPa, 473 K, 10 h).

reaction (1) is given by

$$RT \ln p_{H_2}^{1/2} = \Delta H_H - T\Delta S_H. \tag{2}$$

ΔH_H and ΔS_H are obtained from the slopes and intercepts of plots of $\frac{1}{2}R\ln p_{H_2}$ against $1/T$ at a given r [29]. These were determined after the alloys were subjected to several different HHTs. One set of p–c–T data was determined by one investigator and the other set by a different investigator using a $Pd_{0.81}Au_{0.19}$ alloy subjected to somewhat greater conditions of HHT, 100 MPa. Data were also determined calorimetrically and will be described below. All of the measurements found similar trends.

3.2.5. ΔH_H against r relations. The results for the determinations carried out by the second investigator, including the alloys subjected to the greatest degree of HHT (100 MPa, 473 K), are shown in figure 6. The ΔH_H values are increasingly negative as the degree of HHT increases, i.e. ordering. The ΔH_H values are more exothermic for the HHTed alloy than for the disordered one, which may reflect the more negative H–H interaction energy and more Pd_6 interstices in the ordered structure. There is clearly no plateau in this temperature range, $\geqslant 323$ K, because otherwise ΔH_H would be constant across the 'plateau' region.

   The ΔH_H exhibit minima which shift to larger values of r with increasing degree of HHT (figure 6). Such a minimum is also found for Pd–H, above T_c, but at a larger H content, $r = 0.5$ [30].

   The extended linear decrease of ΔH_H in the alloy subject to the greatest degree of HHT (100 MPa, 473 K, 62 h) (figure 6) arises from an additive term to the H chemical potential, $h_1 \times r$, where h_1 is a constant reflecting an H–H attractive interaction and h_1 must be constant over the linear range. This could be due to the occupation of the favourable Pd-rich octahedral sites in the ordered lattice whose spacings are favourable for the H–H attraction while repulsion is nil because the H–H atoms are sufficiently far apart. The H–H attractive interaction, which is also found in Pd–H and other Pd-rich alloys [23, 30], arises from the elastic interaction between defects in a finite medium [31, 32] and from short range configurational interactions [33]. $h_1 = (\partial \Delta H_H / \partial r)_T = -21.4$ kJ mol^{-1} H for the alloy with the greatest degree of HHT (100 MPa H$_2$, 473 K) (figure 6). Such a linear region is not found for the disordered $Pd_{0.81}Au_{0.19}$ alloy where the slopes change nearly continuously (figure 6), presumably due to the occupation of interstices with varying nearest neighbour environments.
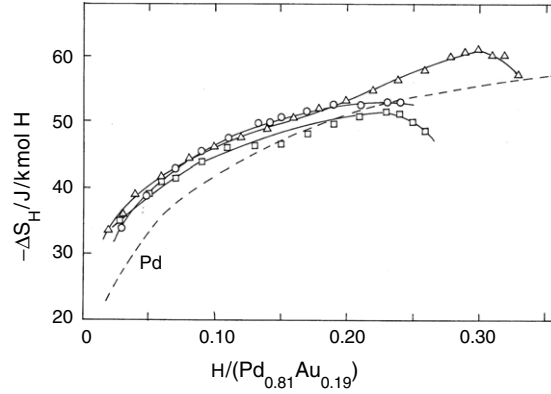
Figure 7. ΔS_H values for several forms of the $Pd_{0.81}Au_{0.19}$ alloy derived from the isotherms shown in figure 5. $\bigcirc$, annealed and slowly cooled; $\square$, HHTed (10.8 MPa, 473 K, 62 h); $\triangle$, HHTed (100 MPa, 473 K, 10 h).

The increase of ΔH_H after the minimum is probably due to the onset of the occupation of a greater number, but energetically less favourable, interstices because an electronic effect due to band filling would be expected to be similar for the various forms of an alloy having the same stoichiometry and therefore the location of the minimum would not shift. The slopes, $(\partial \Delta H_H / \partial r)_T$, at r greater than the minima, are greater for the more ordered alloy (figure 6); i.e., after the minima, $(\partial \Delta H_H / \partial r)_T$ increases with degree of HHT. This might be expected because in the more ordered structure the change with increase of r from the occupation of favourable sites to less favourable ones will occur over a smaller r range than for less ordered structures.

3.2.6. ΔS_H against r relations. ΔS_H versus r relationships for the HHTed alloys are shown in figure 7 along with data for Pd–H, which, because of its plateau, have been obtained from data above its critical point [30]. $(\partial \Delta S_H / \partial r)_T$ values for the HHTed (100 MPa, 473 K) alloy are nearly constant, ≈ -85 J K^{-1} mol^{-1} H, over the same range where $(\partial \Delta H_H / \partial r)_T$ is constant with r and the ΔS_H values increase at about the same r_{min} where ΔH_H increases (figure 6). This is consistent with the increase in availability of interstices at r_{min} which are less energetically favourable than those occupied in the linear region. The entropies for the alloy are more negative than for Pd–H, at least up to about $r = 0.12$, indicating that fewer interstices are available for occupation in the alloy.

The H chemical potential relative to H_2 (0.1 MPa) can be written for low H contents as [29]

$$RT \ln p_{H_2}^{1/2} = \Delta \mu_H = \Delta \mu_H^\circ + RT \ln(r/(\beta - r)) + g_1 \times r, \qquad (3)$$

where $\Delta \mu_H^\circ = \mu_H - \frac{1}{2}\mu_{H_2}$ and $g_1 = h_1 - T s_1$, where the subscript 1 indicates the linear terms in the expansion of $\mu_H^E(r)$ in r.

For the ΔH_H–r plots the slopes are h_1 and for ΔS_H the slope is s_1 plus the ideal partial entropy contribution, $-R(\partial \ln(r/(\beta - r)/\partial r)$. β is the number of available octahedral interstices at a given temperature and p_{H_2}, and it is unity for Pd but less than unity for the Pd–Au alloys because H tends to avoid Au nearest neighbours [10]. If β is chosen as 0.39 for the alloy with the greatest HHT (figure 7) and $s_1 = -16.7$ J K^{-1} mol^{-1} H, the linearity in figure 7 is reasonably well reproduced from $r = 0.1$ to 0.25. The ΔS_H values increase after the minima because more, but energetically less favourable, interstices become available.

9

Table 1. Thermodynamic quantities for hydrogen solution in various forms of $Pd_{0.81}Au_{0.19}$ and pure Pd. ΔH_H and ΔS_H values are in kJ mol$^{-1}\frac{1}{2}$H$_2$, and J K^{-1} mol$^{-1}\frac{1}{2}$H$_2$, respectively, and g_1 is in kJ mol$^{-1}\frac{1}{2}$H$_2$ at 323 K. (Note: The entries in parentheses for ΔH_H° have been determined from plots of $\Delta\mu_H^\circ/T$ against $1/T$ which have been determined from intercepts of $RT\ln p^{1/2}(1-r)/r$ against r and the values without parenthesis from extrapolation of values of ΔH_H and ΔS_H° to $r=0$. β is the fraction of octahedral interstices available for occupancy calculated using the value of ΔS_H assuming $\beta = 1$ and $\Delta S_H^\circ = -55$ J K^{-1} mol^{-1} H (for Pd–H).)

Alloy history	$-\Delta H_H^\circ$	$-\Delta S_H^\circ$ ($\beta = 1.0$)	β	g_1 ($\beta = 1.0$)
Annealed Pd	10.0	55.0	1.0	−46.0
Disordered alloy	15.3(15.2)	59.2	0.60	−28.0
HTT(10.8 MPa)	17.8(17.0)	64.5	0.32	−26.4
HTT(100 MPa)	18.5(17.8)	66.6	0.25	−24.5

3.2.7. Thermodynamic parameters at infinite dilution, ΔH_H° and ΔS_H°. At low H contents the excess chemical potential, $\mu_H^E(r)$, has been replaced in equation (3) by the linear term, $g_1 \times r$, in a polynomial expansion of $\mu_H^E(r)$. Values of g_1 are obtained from the slopes of plots of $RT\ln p_{H_2}^{1/2}(\beta - r)/r$ against r, while the intercepts give $\Delta\mu_H^\circ(= \Delta H_H^\circ - T\Delta S_H^\circ)$. The temperature dependence of $\Delta\mu_H^\circ/T$ gives thermodynamic parameters for hydrogen solution at infinite dilution, ΔH_H° and ΔS_H° (table 1). The thermodynamic parameters at infinite dilution are also shown for Pd–H in table 1, where it can be seen that for all of the forms of $Pd_{0.81}Au_{0.19}$ alloy the enthalpies are more exothermic and $|g_1|$ is smaller than for Pd–H. The values of g_1 in table 1 have been evaluated using $\beta = 1$, and if this is changed to 0.25 for the alloy subject to HHT at 100 MPa g_1 becomes about -34.5 kJ mol^{-1}. In either case, the values are less negative than for Pd–H.

Values of ΔH_H° can also be obtained by extrapolation of the $\Delta H_H(r)$ to $r = 0$ (table 1). The values obtained by the two methods are in reasonable agreement. Since the molar volumes of the various forms of $Pd_{0.81}Au_{0.19}$ are closely similar, the values at infinite dilution are unlikely to be related to the interstice volumes. Not all of the interstices will be occupied in the $Pd_{0.81}Au_{0.19}$ alloy as $r \to 0$. The fraction of preferred octahedral interstices, β, can be estimated by assuming that $\Delta S_H^\circ = -55$ J K^{-1} mol^{-1} H, i.e. the value at infinite dilution of Pd–H, and therefore

$$-55 = \Delta S_H^\circ - R\ln\beta. \tag{4}$$

There is some precedence for assuming that the non-configurational ΔS_H° for the alloy is the same as for Pd–H [34]. Equation (4) gives the values of β shown in table 1, which are valid as $r \to 0$ but are obviously not appropriate at higher p_{H_2} for the alloys after HHTing since H contents larger than the βs can be obtained.

3.3. Dependence of ordering on p_{H_2}, T and time

It will be assumed that the increase in r resulting from HHT, Δr, at a given p_{H_2} in the diagnostic isotherms, is proportional to the degree of ordering introduced. This is analogous to the frequent assumption that decreases of electric resistivity of disordered alloys are quantitatively indicative of ordering.

3.3.1. Time dependence of ordering. Figure 8 shows the effect of the time of the application of HHT at $p_{H_2} = 7.0$ MPa (423 K) on the diagnostic isotherms of an initially disordered alloy. This relatively low temperature for HHT was chosen because ordering is too fast at, e.g., 473 K, which would make the time dependence difficult to follow. At a given p_{H_2} in the diagnostic
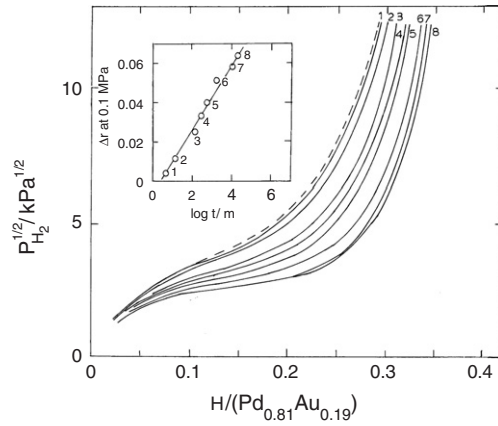
Figure 8. Diagnostic isotherms (348 K) measured as a function of the time of HHT at 423 K, 7.0 MPa. - - - -, annealed $Pd_{0.81}Au_{0.19}$ alloy; 1, 5 min; 2, 15 min; 3, 2.5 h; 4, 5 h: 5, 10 h; 6, 30 h; 7, 18.7 h; 8, 383 h.
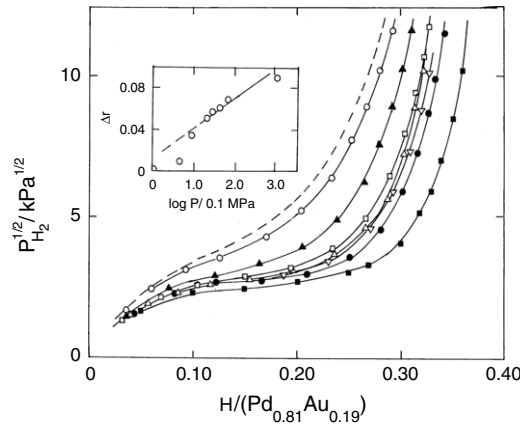
Figure 9. Diagnostic isotherms (348 K) for the $Pd_{0.81}Au_{0.19}$ alloy following HHT (473 K, $\approx$10 h) at different p_{H_2} values. - - - -, annealed alloy; $\bigcirc$, 0.5 MPa; $\blacktriangle$, 1.0 MPa; $\square$, 2.0 MPa; $\triangle$, 3.0 MPa; $\triangledown$, 5.0 MPa; $\bullet$, 7.0 MPa; $\blacksquare$, 100 MPa.

isotherms (348 K), Δr is seen to shift to higher H contents with increase in the time of HHT. A plot of Δr against log t is shown in the inset to be relatively linear, where Δr is the increase in r at 0.1 MPa in the diagnostic isotherms. It should be realized that the fraction of long range order, even after long times at these conditions, is not complete, judging from TEM.

3.3.2. Pressure dependence of ordering at 473 K. It appears that there is an enhancement of the ordering rate in the presence of H_2 because a given fraction of reaction, α, calculated from

$$\alpha = \left(\frac{\Delta r_t}{\Delta r_\infty} \right)_{p_{H_2}, T} \tag{5}$$

appears to be attained faster at higher p_{H_2}, where $\Delta r_t = r$(after HHT) $- r$(before HHT) at $p_{H_2} = 0.1$ MPa and Δr_∞ is the value reached at equilibrium for the given p_{H_2}.

Figure 9 shows complete diagnostic isotherms (348 K) for the $Pd_{0.81}Au_{0.19}$ alloy after HHT of the disordered alloy at 473 K for sufficient times for equilibrium to be reached at each p_{H_2}.
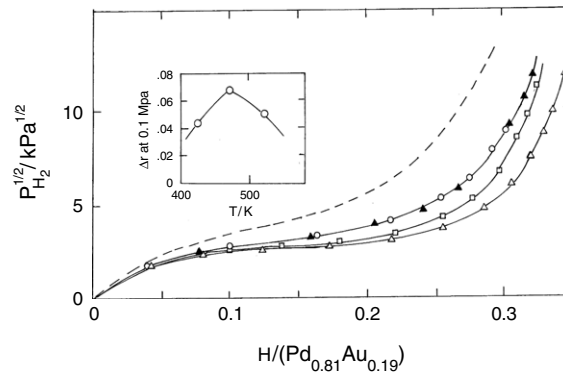
Figure 10. Diagnostic isotherms (348 K) for the $Pd_{0.81}Au_{0.19}$ alloy following HHT at different temperatures (7.0 MPa, ≈10 h). - - - -, annealed $Pd_{0.81}Au_{0.19}$ alloy; O, 598 K; ▲, 423 K; □, 523 K; △, 473 K.

It can be seen that after HHT there is an increase in H_2 solubility with increase of p_{H_2}. The inset shows a plot of Δr versus log p_{H_2}, where the p_{H_2} is that employed for the HHT. There is a nearly linear relationship for intermediate p_{H_2} (figure 9), but at lower p_{H_2} there is a negligible effect of the HHT and, at higher p_{H_2}, the effect levels off.

Wicke and Nernst [23] found for the solubility of H_2 in Pd that the relation log $p_{H_2} = -A(T) + B(T)r$ is followed in the single hydride phase region. A similar relation is found here from ≈1.0 to 7.0 MPa for HHTed $Pd_{0.81}Au_{0.19}$ alloys and, on this basis, the linear relation shown in the inset up to ≈7.0 MPa (figure 9) may be due to the direct dependence of the ordering on the H content during HHT; for lower and higher p_{H_2} this relation is no longer followed. Very high p_{H_2} values with their correspondingly high H contents would be required to attain complete long range ordering.

3.3.3. Temperature dependence of ordering at constant p_{H_2} and time. Figure 10 shows complete isotherms at 348 K following HHT at different temperatures for 10 h at ≈1.0 MPa. It can be seen in the inset that the effect of temperature is a maximum at about 473 K. The maximum arises from two competing effects: (i) an increase in the metal atom diffusion with temperature and (ii) a decrease of hydrogen concentration with temperature at constant p_{H_2}, which decreases the ordering due to less stabilization of the ordered structure by H.

3.3.4. Estimation of the activation energy. Although the rate law for the HHT ordering is unknown, activation energies can, nonetheless, be estimated from the times needed to reach a given fraction of reaction, t_α, for different temperatures at a given $p_{H_2} = 5.0$ MPa. The following equation can be employed for this purpose [25]:

$$\ln t_\alpha = c_1 + \ln A + E_d/RT, \tag{6}$$

where c_1 is a constant. Plots according to equation (7) are shown in figure 11 at different α values, which all give $E_d = 103 \pm 8$ kJ mol^{-1}, which is much smaller than that of 264 kJ mol^{-1} given for the $Pd_{0.5}Au_{0.5}$ alloy by Kohl *et al* [3] or 266 kJ mol^{-1} for pure Pd [35]. Conditions of constant p_{H_2} employed here do not lead to constant r, and therefore there will be a contribution to E_D from the changing H concentration with temperature. This changing concentration would lead to a contribution of ΔH_H in the observed E_D; this would increase it by ≈20 kJ mol^{-1} H
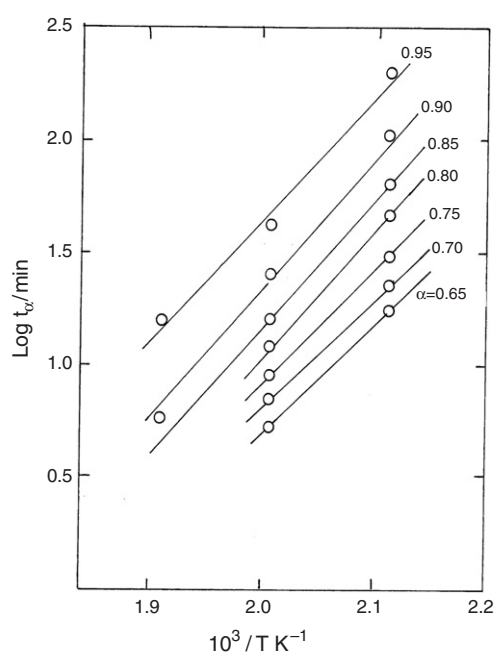
Figure 11. Plots of log t_α for different α values plotted against $1/T$ at 5.0 MPa based on diagnostic isotherms at 348 K. The slopes give E_d/R.

and it would then be close to the 130 kJ mol^{-1} H given by Kohl *et al* for the metal atom mobility only in Pd$_{0.50}$Au$_{0.50}$ [3].

The small value of E_D found here is compatible with the observation that the ordering takes place at relatively moderate temperatures, e.g. 423 K. The dissolved H may lower the activation energy [19] and/or create vacancies [36, 37], as has been suggested in the literature for pure Pd and Pd–Rh alloys.

3.4. The ordered → disordered transformation

A disordered Pd$_{0.81}$Au$_{0.19}$ alloy was ordered under HHT (523 K, 7.0 MPa, 190 h) and then annealed *in vacuo* at 523 K. This caused it to revert to its disordered form, as shown by its diagnostic isotherm, which was nearly that characteristic of its disordered form (figure 12). This is an important finding, because it proves that the ordered state is not thermodynamically stable *in the absence of dissolved hydrogen*.

Some other annealing experiments were carried out in the presence of 1.0 MPa H$_2$ rather than *in vacuo*. The disordered alloy was prepared by annealing at 1173 K *in vacuo* for 5 h and it was then HHTed at 523 K for 41 h at 10.0 MPa H$_2$. The resulting ordered alloy was then heated at 523 K, i.e. the same temperature as used for HHT, in 1.0 MPa H$_2$ rather than in 10 MPa, where more ordering took place. After a series of anneals at 523 K at 1.0 MPa, its diagnostic isotherms (348 K) progressively return towards that of the disordered form (figure 13), although, because of the 1.0 MPa H$_2$, it did not return all the way to the isotherm characteristic of the disordered form but to one found for the initially disordered alloy which had been subjected to HHT in 1.0 MPa H$_2$. These results are shown in figure 13, compared to a disordered alloy which had been subject to HHT at 1.0 MPa for 2440 h.
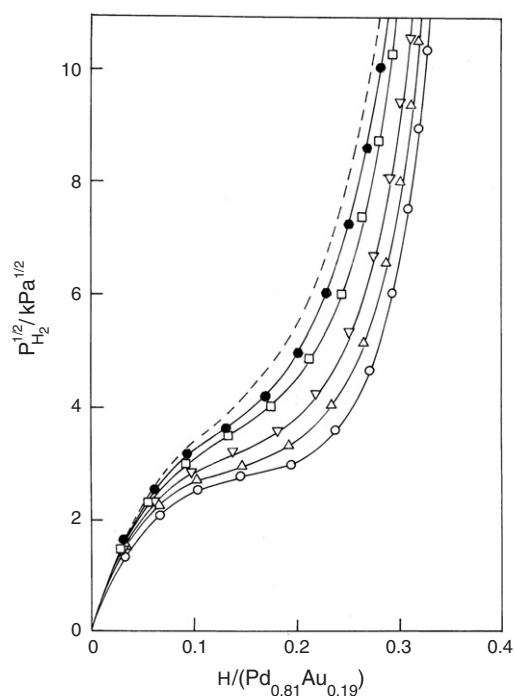
Figure 12. Diagnostic isotherms (348 K) reflecting the annealing *in vacuo* (523 K) of an initially HHTed (10 MPa, 523 K, 41 h) $Pd_{0.81}Au_{0.19}$ alloy. - - - -, annealed alloy; $\triangle$, 13.5 h; $\triangledown$, 30 h; $\square$, 83.5 h; $\bullet$, 195 h.

This experiment (figure 13) demonstrates that starting from either form of the alloy, i.e. ordered or disordered, after prolonged treatment in 1.0 MPa H_2(g), 523 K, their diagnostic isotherms become almost the same. Since the same state is approached from either direction, the final state must be close to equilibrium for conditions of 1.0 MPa of H_2(g) (523 K). This shows that equilibrium is reached at different p_{H_2} conditions such as shown in figure 9.

Another conclusion which can be drawn from these annealing experiments (figures 12, 13) is that the return to the equilibrium state characteristic of 1.0 MPa H_2(g) (523 K) takes place faster in H_2 than *in vacuo*, at least for shorter annealing times, demonstrating that dissolved hydrogen enhances the rate of metal atom rearrangement, as found elsewhere for Pd alloys, e.g. [18].

3.5. Calorimetric determinations of ΔH_H and ΔS_H

Reaction calorimetry was carried out (303 K) for both the HHTed (100 MPa at 523 K for 4 h) and the annealed $Pd_{0.81}Au_{0.19}$ alloy forms. Isotherms at a lower temperature, 303 K, than the 348 K employed above are shown for both forms of the alloy in figure 14, where there is seen to be a larger difference between the two forms of the alloy than for the higher temperatures (figure 5). Both absorption and desorption were measured and there is no indication of hysteresis at this temperature for either the disordered or ordered alloy forms.

It is difficult to reconcile the very large increase in solubility (figure 14) with the relatively small fraction of the super-lattice phase which forms under these conditions of HHT as shown in figure 1; however, for the reasons pointed out above, ordering must be the cause of the
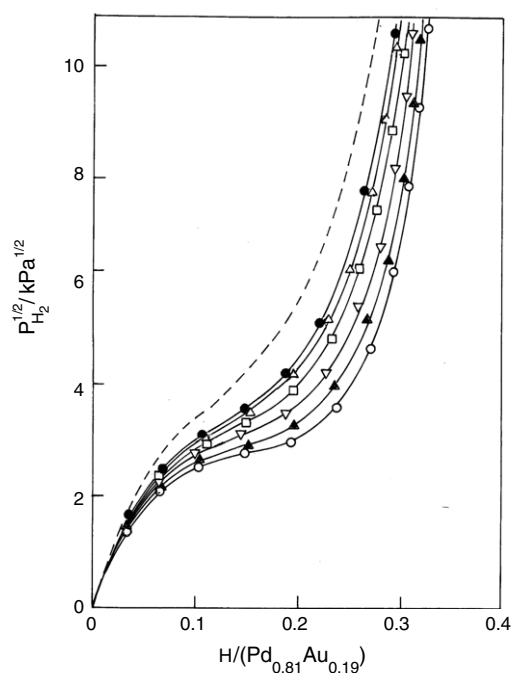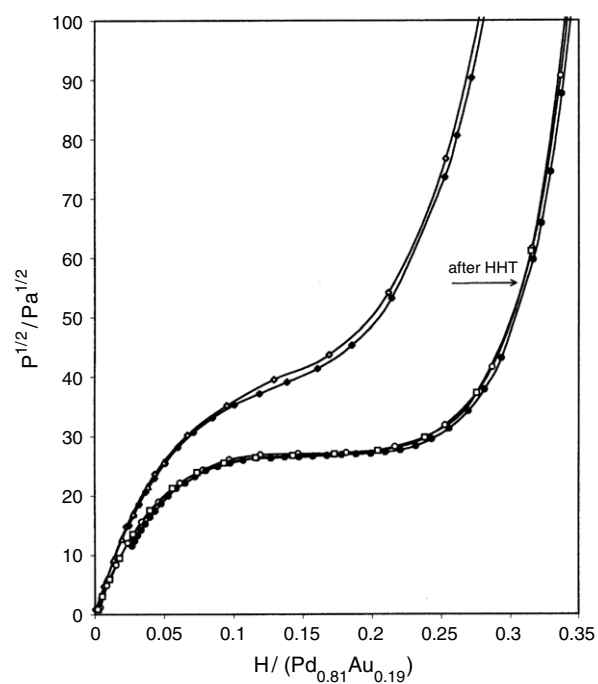
Figure 13. Diagnostic isotherms (348 K) for the annealing in 1.0 MPa H_2 (523 K) of an initially HHTed $Pd_{0.81}Au_{0.19}$ alloy and initially disordered $Pd_{0.81}Au_{0.19}$ alloy. - - - -, disordered $Pd_{0.81}Au_{0.19}$ alloy; ●, HHTed 41 h in 1.0 MPa initially disordered $Pd_{0.81}Au_{0.19}$ alloy; ▲, HHTed 4 h in 1.0 MPa H_2 initially ordered alloy; ▽, HHTed 17 h in 1.0 MPa H_2 ordered alloy; □, HHTed 47 h in 1.0 MPa H_2 ordered alloy; △, HHTed 194 h in 1.0 MPa H_2 ordered alloy.

enhanced solubilities and therefore short range order may also be contributing to the solubility increases.

The calorimetric technique is more reliable for determining ΔH_H values than the p–c–T method in the high H content regions, and therefore these determinations were carried out to verify the above results. The ΔH_H–r relationships for the HHTed (100 MPa at 523 K for 4 h) alloy were determined calorimetrically (303 K) along with the equilibrium p_{H_2}, which gives ΔS_H values of $\Delta S_H = \Delta H_H/T - R \ln p_{H_2}^{1/2}$. The ΔH_H values are shown for both forms in figure 15, where there is a minimum of about -24 kJ mol^{-1} H at $r = 0.29$ for the HHTed form and a broader minimum for the disordered form with -22 kJ mol^{-1} H. These agree quite well with the values based on the p–c–T measurements (figure 6). It appears from the isotherms (figures 5 and 14) that there may be a plateau for the HHTed form, but, since neither the enthalpies or entropies (figure 16) are constant as expected for a two phase plateau region, there is no plateau. The enthalpies decrease nearly linearly from about $r = 0.10$ to 0.25 as noted earlier (figure 5). ΔS_H values are shown for both forms in figure 16.

In order for p_{H_2} to be nearly constant as it is for the HHTed alloy at 303 K (figure 14) in the region where ΔH_H decreases linearly with r, $-T\Delta S_H$ must increase directly with r as seen (figure 16). This is consistent with a physical picture of a limited number of favourable sites being occupied where the H–H interaction energy causes ΔH_H to become more negative and ΔS_H more negative as these sites are occupied. This compensation effect is of interest because apparent two phase plateau regions based only on a nearly constant p_{H_2} are seen to be misleading. Such a compensation effect has been noted for H_2 solution in Pd–Mn alloys [38].
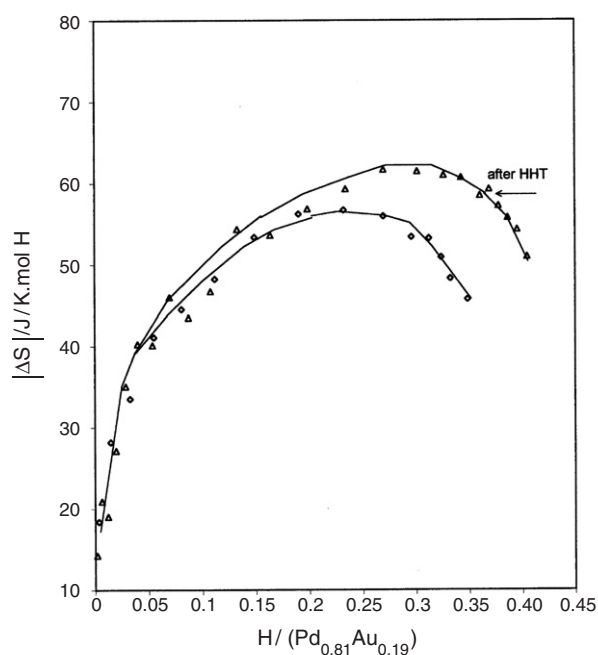
Figure 14. Diagnostic isotherms (303 K) for the $Pd_{0.81}Au_{0.19}$ alloy before and after HHT (100 MPa, 523 K, 4 h). The open and filled symbols are for absorption and desorption of H_2, respectively.
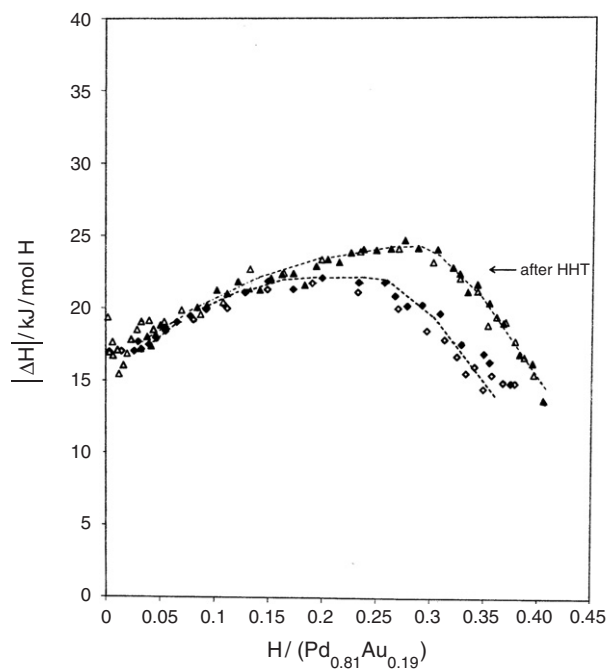
Figure 15. Calorimetrically determined ΔH_H values (303 K) measured before and after HHT (100 MPa, 523 K, 4 h). The empty and filled symbols refer to absorption and desorption of H_2, respectively.

16

Figure 16. Calorimetric ΔS_H values (303 K) measured during absorption before and after HHT (100 MPa, 523 K, 4 h). The empty and filled symbols refer to absorption and desorption of H_2, respectively.

3.6. Conclusions

This is an illustration of the use of hydrogen solubilities for following lattice changes in Pd alloys. Although physical techniques such as TEM also indicate lattice changes, their sensitivity is usually not as great as H_2 solubilities. The ordering of $Pd_{0.81}Au_{0.19}$ alloys takes place under the influence of dissolved hydrogen at moderate temperatures. Dissolved H is shown to stabilize the ordered structure because the alloy reverts to its disordered form upon annealing *in vacuo* at the same temperatures as employed for the HHT ordering. This is consistent with the results of Kawasaki *et al* [4], who suggested that a bulk alloy does not order *in vacuo*, however, the reasons differ. The present work using bulk alloys suggests that the ordered state is not thermodynamically stable in the absence of dissolved H, whereas Kawaskai *et al* suggest the bulk does not order for kinetic reasons.

Relatively large concentrations of hydrogen are required to stabilize the ordered structure, because when the rearranged alloy is annealed at 523 K or higher it reverts to its original disordered structure. It is also shown that dissolved H enhances the metal atom diffusion leading to ordering/disordering.

Acknowledgments

References

[1] Okamoto H and Massalski T 1985 *Bull. Alloy Phase Diagrams* **6** 229
[2] Copeland W and Nicholson M 1964 *Acta Metall.* **12** 321

  [3] Kohl W, Mais B and Lücke K 1987 *Mater. Sci. Forum* **15–18** 1219
  [4] Kawasaki Y, Ino S and Ogawa S 1971 *J. Phys. Soc. Japan* **30** 1758
  [5] Darby J 1966 *Acta Metall.* **14** 265
  [6] Lee S-M, Flanagan T and Kim G-H 1995 *Scr. Metall. Mater.* **32**
  [7] Lovvick O and Olsen R 2002 *J. Alloys Compounds* **330–332** 332
  [8] Allard K, Maeland A, Simon J and Flanagan T 1968 *J. Phys. Chem.* **72** 136
  [9] Shamsuddin M and Kleppa O J 1979 *J. Chem. Phys.* **71** 5154
 [10] Wagner F, Karger M, Pröbst F and Schüttler B 1983 *Electronic Structure and Properties of Hydrogen in Metals*
          ed P Jena and C Satterthwaite (New York: Plenum) p 581
 [11] Noh H, Flanagan T and Ransick M 1992 *Scr. Metall. Mater.* **26** 353
 [12] Noh H, Clewley C and Flanagan T 1996 *Scr. Metall.* **34** 665
 [13] Noh H, Clewley J D, Flanagan T B and Craft A 1996 *J. Less-Common Met.* **240** 235
 [14] Flanagan T, Craft J, Kuji T, Baba K and Sakamoto Y 1987 *Scr. Metall.* **20** 1745
 [15] Baba K, Niki Y, Sakamoto Y, Flanagan T and Craft A 1987 *Scr. Metall.* **21** 1147
 [16] Ahlzen P, Andersson Y, Tellgren R, Rodic D, Flanagan T and Sakamoto Y 1989 *Z. Phys. Chem. N.F.* **163** 213
 [17] Ahlzen P, Andersson Y, Tellgren R, Rodic D, Flanagan T and Sakamoto Y 1990 unpublished results
 [18] Flanagan T, Noh H, Clewley J and Barker J 1998 *Scr. Mater.* **39** 1607
 [19] Flanagan T and Park C-N 1999 *J. Alloys Compounds* **293–295** 161
 [20] Flanagan T B, Luo W and Clewley J D 1991 *J. Less-Common Met.* **172–174** 42
 [21] Maeland A and Flanagan T 1965 *J. Phys. Chem.* **69** 3575
 [22] Feder R, Mooney M and Nowick A 1958 *Acta Metall.* **6** 266
 [23] Wicke E and Nernst G 1964 *Ber. Bunsenges. Phys. Chem.* **68** 224
 [24] Flanagan T, Clewley J, Noh H, Barker J and Sakamoto Y 1998 *Acta Mater.* **40** 2173
 [25] Burke J 1965 *The Kinetics of Phase Transformations in Metals* 1st edn (Oxford: Pergamon) p 65
 [26] Park C-N and Flanagan T B 1997 *Scr. Mater.* **37** 1709
 [27] Flanagan T B, Majchrzak S and Baranowski B 1972 *Phil. Mag.* **25** 257
 [28] Sakamoto Y, Flanagan T B and Kuji T 1985 *Z. Phys. Chem. N.F.* **143** 61
 [29] Oates W A and Flanagan T B 1981 *Prog. Solid State Chem.* **13** 193
 [30] Kuji T, Oates W, Bowerman B and Flanagan T 1983 *J. Phys. F: Met. Phys.* **13** 1785
 [31] Eshelby J 1956 *Solid State Phys.* **3** 79
 [32] Alefeld G 1972 *Ber. Bunsenges. Phys. Chem.* **76** 746
 [33] Mohri T and Oates W 2002 *Mater. Trans.* **43** 2356
 [34] Chowdhury M and Ross D 1973 *Solid State Commun.* **13** 229
 [35] Peterson N L 1964 *Phys. Rev.* A **136** 568
 [36] Fukai Y, Ishii Y, Goto T and Watanabe K 2000 *J. Alloys Compounds* **313** 121
 [37] Watanabe K, Okuma N, Fukai Y, Sakamoto Y and Hayashi Y 1996 *Scr. Mater.* **34** 551
 [38] Flanagan T and Luo S 2006 *J. Phys. Chem.* B **110** 8080